

# Chitosan hydrogel beads for fulvic acid adsorption: Behaviors and mechanisms

Shu-Guang Wang\*, Xue-Fei Sun, Xian-Wei Liu,  
Wen-Xin Gong, Bao-Yu Gao, Nan Bao

*School of Environmental Science and Engineering, Shandong University, Jinan 250100, China*

Received 14 August 2007; received in revised form 2 November 2007; accepted 19 November 2007

## Abstract

Chitosan hydrogel beads were studied for the adsorption of fulvic acid (FA) from aqueous solutions to examine the adsorption behaviors and mechanisms. Kinetic and isotherm studies were carried out by considering the effects of various parameters, such as initial concentration (5–50 mg/L), temperature (15, 30, 45 °C), pH (4–12) and ionic strength (0–0.5 M NaCl). The results indicate that the adsorption of FA is strongly dependent on pH and ionic strength under our experimental conditions. The adsorption kinetics and isotherms showed that the sorption processes were fitted better by intra-particle model and the Freundlich equation, respectively. Point of zero charge ( $\text{pH}_{\text{PZC}}$ ) study indicated that the surface of chitosan hydrogel beads was positively charged at  $\text{pH} < 9.9$  and negatively charged at  $\text{pH} > 9.9$ . Fourier transform infrared spectroscopy suggested that FA adsorption was mainly through interactions with the N atoms in chitosan hydrogel beads and further X-ray photoelectron spectroscopy (XPS) revealed the formation of organic complex between the protonated amino groups and FA after adsorption.

© 2007 Elsevier B.V. All rights reserved.

*Keywords:* Chitosan hydrogel beads; Fulvic acid; Adsorption; Mechanisms

## 1. Introduction

Humic substances (HS), a major component of organic matter, are some of the most abundant materials on earth. These brownish biopolymers can be found in animals, plants, sediments, soils and waters. Especially, they are a predominant type of an organic matter in natural waters [1,2]. Fulvic acids (FA) comprises over 70% of HS and they are close to being non-biodegradable and are the end-point of nature's biodegradation [3,4]. The presence of FA in water can adversely affect appearance and taste, and they have been shown to be especially reactive with a variety of oxidants and disinfectants used for the purification of drinking water forming disinfection by-products (DBPs), a number of which have been shown to cause cancers in laboratory animals [5,6]. Furthermore, in the ultrafiltration of natural waters in drinking water treatment, decline of the flux is generally experienced in the presence of FA and other humic

substances [7]. So the necessity to remove FA from water in an effective way is great.

Several methods are available for FA removal from drinking water such as ion exchange, ultrafiltration, adsorption by clay, active carbon, aluminas and coagulation using chemicals such as ferric salts [8–13]. Among them, adsorption is regarded as a promising one for the removal of these substances. So, it is very necessary and significant to explore new adsorbents with high adsorption capacity and efficiency to remove FA from water.

One potential adsorbent material can be chitosan, which is a copolymer of 2-glucosamine and *N*-acetyl-2-glucosamine, derived from chitin, by deacetylation reaction in hot alkali [14]. Because of its macromolecular structure, chitosan exhibits many characteristics that have been the cause of much recent attention. Many researchers have explored the possibility of using chitosan for dye and metal cation removal [15–19]. These studies have shown that chitosan exhibits good adsorption capacity for these compounds since its amino and hydroxyl groups can act as chelating sites. Whereas, limited reports have been found in the literature on treatment of FA by chitosan [14]. Furthermore, through the gel formation process, chitosan hydrogel beads could improve the adsorption capacity of chitosan by reducing

\* Corresponding author. Tel.: +86 531 88362802; fax: +86 531 88364513.

*E-mail addresses:* [wsg@sdu.edu.cn](mailto:wsg@sdu.edu.cn) (S.-G. Wang), [xfsun06@gmail.com](mailto:xfsun06@gmail.com) (X.-F. Sun).

the crystallinity [15] and further they can be separated easily after adsorption. Thus, there is an urgent need to investigate the removal capacity and mechanisms of chitosan hydrogel beads during the removal of organic matter.

Therefore, the main objectives of our research are (1) to characterize chitosan hydrogel bead and its reaction products before and after reaction with FA; (2) to investigate FA removal by chitosan hydrogel beads at different pH conditions, temperature, time and the effect of ionic strength; (3) and to identify the adsorption mechanisms, using Fourier transform infrared spectroscopy (FTIR), X-ray photoelectron spectroscopy (XPS) spectra and the point of zero charge (PZC) analysis.

## 2. Experimental

### 2.1. Materials and chemicals

Chitosan flakes (85% deacetylated) used in the experiments were purchased from Sinopharm Chemical Reagent Co., Ltd., Shanghai, China. FA was obtained from the Institute of Coal Chemistry, Chinese Academy of Sciences. Though the exact chemical structure of FA is variable and not available, it is known to be a high molecule containing a large number of reactive functional groups (e.g., carboxylic group, phenolic group) [17]. All other chemicals were of reagent grade purity and all chemical stock solutions were prepared using Deionized (DI) water and were stored at 4 °C.

### 2.2. Preparation of chitosan hydrogel beads

One-gram chitosan flakes were added into 50 mL 2% (v/v) acetic acid in a beaker to obtain chitosan solution and the mixture placed overnight. Then the chitosan solution was dropped through a syringe needle into 100 mL 3% (w/v) sodium hydroxide with 1.5 mL ethyl acetate solution to induce the formation of spherical gel beads, mechanically stirred for 3 h. After removing the sodium hydroxide solution, the beads were washed with DI water repeatedly until reaching neutrality and they were stored in DI water for further use.

### 2.3. Chitosan hydrogel beads surface morphology observation

For surface morphologies samplings, FA was first treated with chitosan hydrogel beads for 45 h, and then the treated solutions were centrifuged and the precipitate was dried at 40 °C for 7 days. The samples were examined with a scanning electron microscope (SEM, S-520, Hitachi, Japan), and the lyophilized sample coated in a JEOL JFC-1300 Auto Fine Coater fitted with Pt target before the observation.

### 2.4. FTIR spectroscopy

FTIR spectra of chitosan hydrogel beads and chitosan hydrogel bead-treated FA complexes were recorded using FTIR (Aratar, Thermo-NicoLet, USA) connected with a personal computer. FTIR spectra were measured on KBr pellets prepared by

pressing mixtures of 1 mg dry powdered sample and 100 mg spectrometry grade KBr under a vacuum, with precautions taken to avoid moisture uptake.

### 2.5. XPS analysis

The surfaces of chitosan hydrogel beads and FA-laden chitosan hydrogel beads were analyzed using XPS (PHI 5300, USA) with an Al KR X-ray source (1486.71 eV of photons). The X-ray source was run at a reduced power of 150 W, and the pressure in the analysis chamber was maintained at less than  $10^{-8}$  Torr during each measurement. All binding energies were referenced to the neutral C 1s peak at 284.6 eV to compensate for surface charging effects. A software package, XPS peak 4.1, was used to fit the XPS spectra peaks, and the full width at half-maximum (FWHM) was maintained at 1.4 for all components in a particular spectrum.

### 2.6. PZC analysis

Determination of PZC of chitosan hydrogel beads was performed according to the method described in the literature [18]. The mixture of 2 g of chitosan hydrogel beads and 100 mL of 0.1 M potassium nitrate solution was agitated in a closed Erlenmeyer flask at 25 °C for 24 h to allow it to reach the equilibrium state. The initial pH ( $\text{pH}_i$ ) was adjusted to a value between 4 and 12 by adding 0.1 M  $\text{HNO}_3$  or 0.1 M KOH solutions. The graphs of final pH ( $\text{pH}_f$ ) versus  $\text{pH}_i$  were used to determine the PZC of chitosan hydrogel beads.

### 2.7. Experimental procedure

#### 2.7.1. Kinetic experiments

Batch kinetic experiments were performed by mixing a fixed amount of sorbent (20 g/L) with 2 L FA solution of different concentration. The mixture was shaken for 45 h, and during this time, samples were collected at fixed intervals. After the spectrophotometric analysis of each sample, the concentration of FA in the aqueous solution at fixed time ( $C_e$ ) was calculated.

#### 2.7.2. Equilibrium experiments

The effect of the initial FA concentration was determined by placing 2 g of chitosan hydrogel beads in contact with 100 mL of aqueous solutions containing different FA concentrations (5–100 mg/L), and the suspensions were shaken for 45 h at natural pH.

The influence of pH on the adsorption process was studied by mixing 2 g of sorbent with 100 mL of aqueous FA solutions of 50 mg/L concentration. The pH of each solution was adjusted using 1 M NaOH and HCl and measured using a pH meter (MP220 pH meter, Mettler-Toledo GmbH, Schwerzenbach, Switzerland). The suspension was shaken for 45 h using a bath to control the temperature at 25 °C. In order to investigate the ionic strength effect, 1 M NaCl solution was added to the FA solution to desired values. Other procedures were the same as those used in the influence of pH experiments.

## 2.8. Analytical methods for FA

The suspension was filtered through 0.45  $\mu\text{m}$  membrane filters and was analyzed using a UV–vis spectrophotometer (model UV754GD, Shanghai) at an absorbance wavelength of 254 nm. The FA concentration was calculated from a calibration curve of absorbance versus concentration.

## 3. Results and discussion

### 3.1. Characterization of chitosan hydrogel beads

Scanning electron micrographs (SEM) of chitosan hydrogel beads are presented in Fig. 1. It is readily observed that chitosan hydrogel bead surface was rugged with surface protuberances (Fig. 1a), but became much smoother after FA adsorption (Fig. 1b), and no obvious pores were observed on chitosan hydrogel bead surface. This predicts that thin layer of the FA has covered the entire external surface of chitosan hydrogel beads.

XPS spectra are widely used to distinguish the different forms of the same element and to identify the existence of a particular element in a material [1]. Fig. 2 shows the typical results of XPS spectra for chitosan hydrogel beads which reveals carbon, oxygen and nitrogen are the predominant elements observed on the surface from binding energies at 284.6 eV (C 1s), 532.3 eV (O 1s) and 399.1 eV (N 1s) with the atomic ratio of C:N:O at 72.59:3.22:24.19. Based upon binding energies, surface moieties of chitosan hydrogel beads are identified as  $-\text{CH}_2\text{OH}$ ,  $-\text{CO}$ , and  $-\text{NH}_2$ .

### 3.2. Point of zero charge (PZC)

The effect of surface functionality on FA adsorption may be complicated by the charge characteristics of chitosan hydrogel bead surface. Over the range of experimental pH values, a portion of surface functional groups should become deprotonated with increasing pH. This results in a less positively

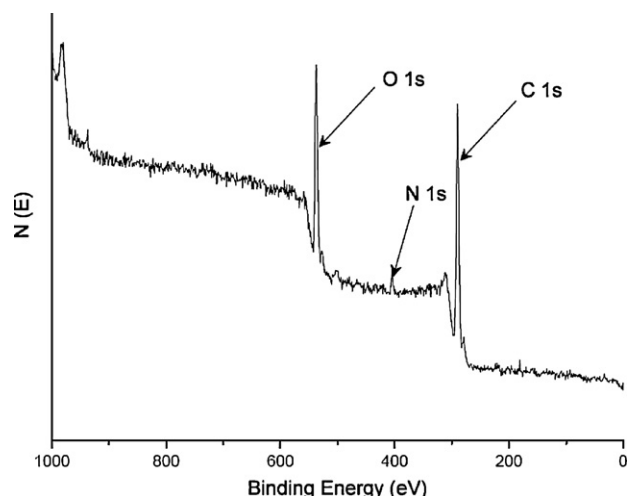


Fig. 2. Typical XPS spectra of chitosan hydrogel bead.

or more negatively charged chitosan hydrogel bead surface at higher pH than at lower pH. Thus, depending on the pH of the solution, their surfaces might be positively charged, negatively charged, or neutral when the solution pH is below, above, or equal to the PZC, respectively [19]. This has been reported for activated carbon cloth [20]. The PZC values were usually discrepant in different studies, which might be attributed to the different preparation and treatment methods [21]. In this study, the PZC of chitosan hydrogel beads was around 9.9 (Fig. 3), indicating that over the experimental pH range a charge reversal from positive to negative on the surface of chitosan hydrogel beads occurred with increasing pH. Such charge properties of chitosan hydrogel bead surface would be expected to have a dramatic effect on the adsorption of FA. Moreover, FA was negatively charged over the whole range of pH studied in general [22]. In this case, the negatively charged FA adsorbed on chitosan hydrogel beads and neutralized the positive charges. As a result, the PZC of FA-coated chitosan hydrogel beads shifted from 9.9 to 6.5.

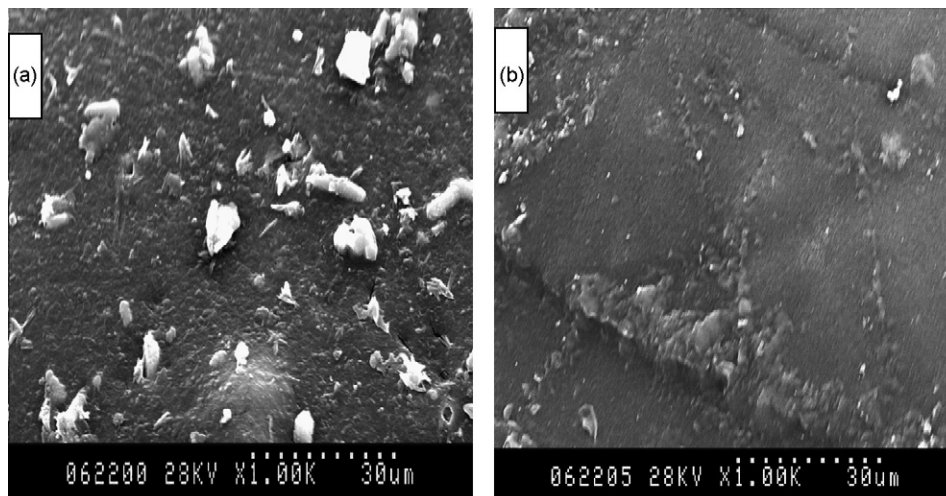


Fig. 1. SEM surface images (a) chitosan hydrogen bead ( $\times 1000$ ) and (b) chitosan hydrogen bead with FA ( $\times 1000$ ).

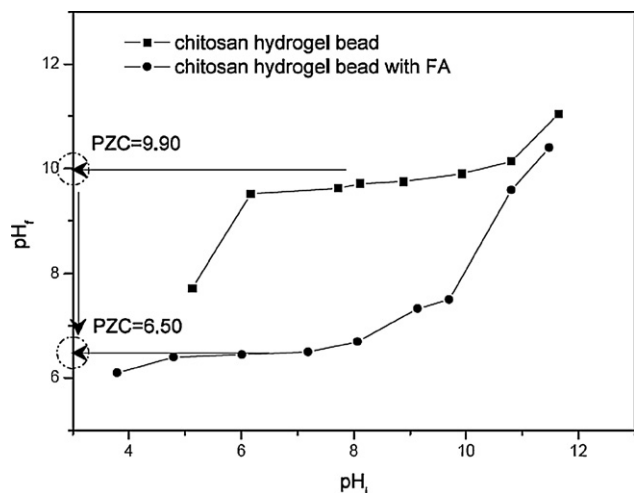


Fig. 3. Determination of  $pH_{PZC}$  of chitosan hydrogel bead in  $KNO_3$  solutions.

### 3.3. Sorption kinetics for FA

To investigate the effect of the FA concentration on the adsorption rate, a series of freshly prepared FA solutions ( $5\text{--}50\text{ mg/L}$ ) of  $pH\ 4.0 \pm 0.02$  were used. Fig. 4 shows a typical result for FA adsorption on chitosan hydrogel beads. As indicated, FA adsorption on chitosan hydrogel beads increases with the increase in initial concentration of FA, and the plots are characterized by a monotonous increasing trend with the steep climb at the beginning of sorption (within 5 h) being succeeded by a more gradual rise (5–31 h), reaching equilibrium at 31 h. The parameters of the pseudo first-order kinetic model and the intra-particle diffusion model are summarized in Table 1. Fig. 4 (inset) depicts the applicability of intra-particle diffusion model on the prediction of adsorption kinetics of FA on chitosan hydrogel beads at different initial concentrations. As is shown, the adsorption of FA onto chitosan hydrogel beads can be considered as two steps process: (1) film or boundary layer diffusion and (2) the intra-particle diffusion. In the ini-

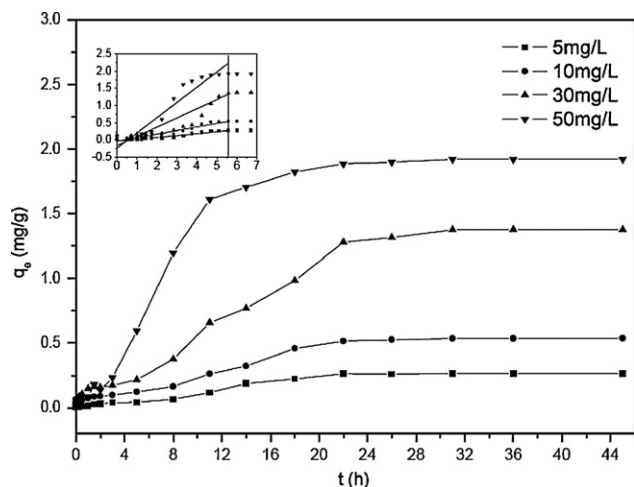


Fig. 4. Effect of the initial concentration on the adsorption behavior of FA on chitosan hydrogel beads.

Table 1

Parameters of adsorption of FA (mg/g) on chitosan hydrogel beads to kinetic model at  $t = 25\text{ }^\circ\text{C}$

Initial concentration (mg/L)	Pseudo first-order kinetic		Intra-particle diffusion	
	$k_1$ (1/min)	$R^2$	$k_{int}$ (mg/g min <sup>1/2</sup> )	$R^2$
5	0.09	0.793	0.059	0.939
10	0.06	0.786	0.110	0.936
30	0.05	0.941	0.280	0.942
50	0.08	0.879	0.438	0.962

tial stage, the adsorbent surface is relatively free of FA and the kinetics of adsorption may be considered as a transport-limited process controlled by the diffusion of FA molecules from the bulk solution to the adsorbent surface, as all the FA molecules that arrive at the adsorbent surface may attach instantly to the protonated amino groups  $-\text{NH}_3^+$  of chitosan hydrogel beads. When overstepping the initial adsorption period, the increasing of adsorption amounts with time was very slow. The adsorption process may become intra-particle diffusion limited due to the unavailability of the active protonated amino groups  $-\text{NH}_3^+$  on the adsorbent surface. Furthermore, the incoming FA molecules also encounter unfavourable electrostatic interactions from the adsorbed FA molecules.

In general, adsorption of FA onto chitosan hydrogel beads follows the intra-particle diffusion model best among various concentrations. The rate constant  $k_{int}$  is shown in Table 1, which increased with increasing initial FA concentration. If intra-particle diffusion is rate-limited then plots of adsorbate uptake  $q_t$  versus the square root of time ( $t^{1/2}$ ) would result in a linear relationship. Moreover, the particle diffusion would be the rate-controlling step if the lines pass through the origin [23]. The curves, as shown in Fig. 4, indicated that the mechanism of FA removal on chitosan hydrogel beads is complex and both the surface adsorption as well as intra-particle diffusion contributes to the rate-determining step [24]. This kinetic model was also used to describe successful experimental data of chitosan flake and activated clay composite beads for the adsorption of HA [25].

### 3.4. Sorption isotherms for FA

Adsorption isotherms describe how adsorbates interact with adsorbents and so are critical in optimizing the use of adsorbents. Therefore, the correlation of equilibrium data by either theoretical or empirical equations is essential to the practical design and operation of adsorption systems [16]. In the present studies, the experimental data obtained at  $pH\ 4.0 \pm 0.02$  were analyzed with the Freundlich and Langmuir equations. The Freundlich equation is an empirical approach for adsorbents with very uneven adsorbing surfaces. This model is applicable to adsorption of a single solute system within a fixed range of concentration [26]. The Langmuir equation was originally developed to describe individual chemical adsorbents, and is applicable to physical adsorption (monolayer) within a low concentration range [26]. The equations of the above two types of sorption isotherms are



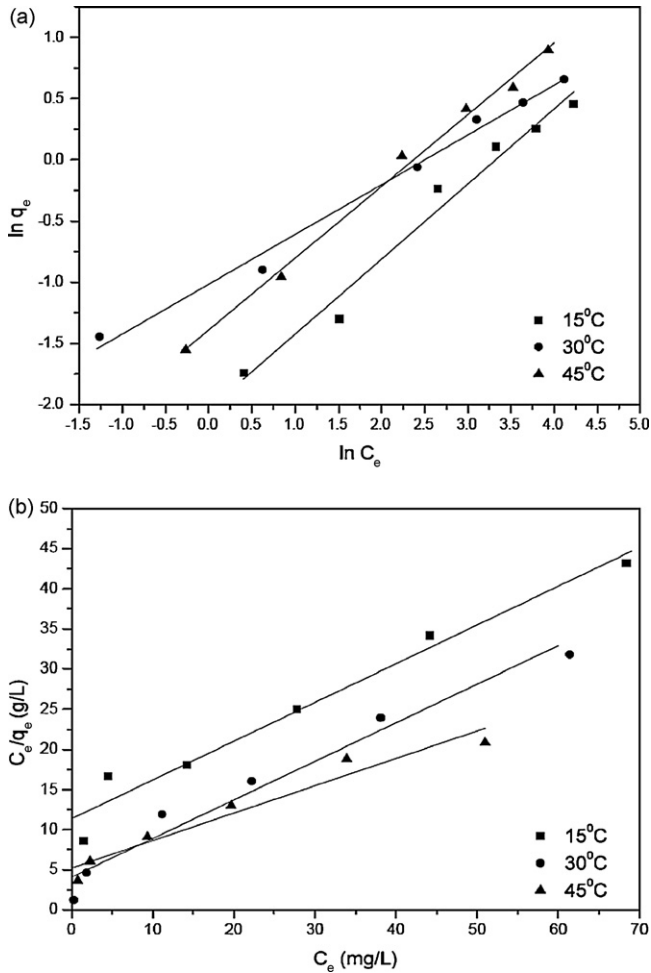


Fig. 5. Linearized adsorption isotherms of (a) Freundlich and (b) Langmuir at various temperatures.

expressed as follow:

$$\ln q_e = \ln K_F + \frac{1}{n}(\ln C_e) \quad (1)$$

$$\frac{C_e}{q_e} = \frac{1}{Q^0 b} + \frac{C_e}{Q^0} \quad (2)$$

where  $q_e$  is equilibrium uptake capacity of chitosan hydrogel beads,  $C_e$  is the concentration of FA in the supernatant after sorption,  $n$  and  $K_F$  are empirical constants,  $Q^0$  and  $b$  are Langmuir's constants related to the capacity and energy of the adsorption. The sorption isotherms are shown in Fig. 5. Sorption equations and their correlation coefficients ( $R^2$ ) are listed in Table 2. The

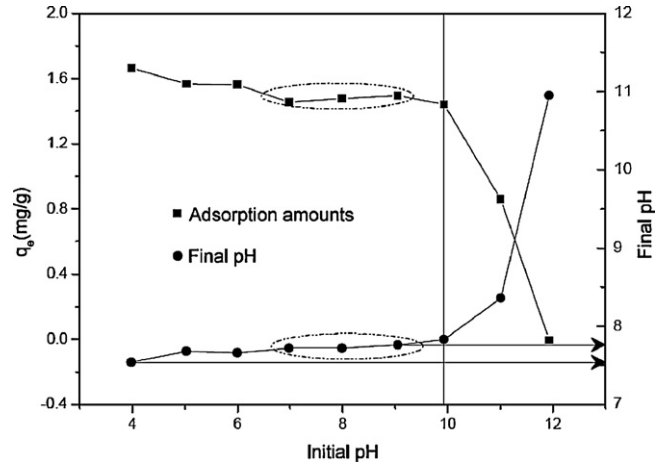


Fig. 6. Effect of pH on FA adsorption onto chitosan hydrogel beads.

results indicate that the Freundlich equation and the Langmuir equation fit well the sorption of FA onto chitosan hydrogel beads, and this shows that the sorption behavior of FA is very complicated and might be affected by many factors. From the data in Table 2, the maximum sorption capacity of FA increased with increasing temperature which increased surface activity and increased kinetic energy of the FA molecules.

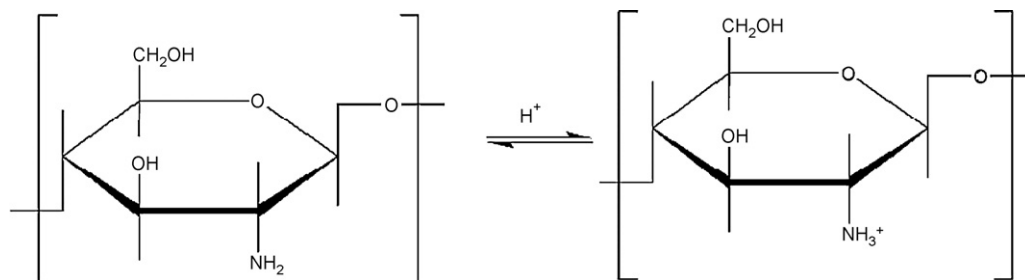
### 3.5. Influence of pH on FA adsorption

It is important to examine the effect of solution pH on adsorption performance as many adsorbents have pH-dependent adsorption performance, and also the natural waters that contain FA usually have different solution pH values. The adsorption results of FA onto chitosan hydrogel beads with the initial concentration of 50 mg/L is shown in Fig. 6, with variations in the initial pH and final pH causing corresponding changes in the reacted solution. Chitosan hydrogel beads showed a pH-dependent adsorption behavior and the adsorption capacity is greater at low pH and decreases with increasing pH. This trend was also observed for fulvic and polymaleic acid adsorption on goethite [27], for comparing humic acid (HA) adsorption at pH 3 and 9 on hematite [28] and for HS adsorption onto kaolinite and hematite [29].

The phenomena is interpreted that at low solution pH values, the functional groups ( $-\text{NH}_2$ ) on the surface of chitosan hydrogel beads can react with the hydrogen ions in the solutions, and the resultant surface complexes cause chitosan hydrogel beads to have positive surface charges. As illustrated in Scheme 1, a

Table 2  
Equations of sorption isotherms of FA onto chitosan hydrogel beads at different Temperature

$T$ ( $^{\circ}\text{C}$ )	Freundlich		Langmuir		
	Model	$R^2$	Model	$R^2$	$Q^0$
15	$\ln q_e = 0.483 \cdot \ln C_e + 11.343$	0.978	$\frac{C_e}{q_e} = 0.614 \cdot C_e - 2.037$	0.968	2.069
30	$\ln q_e = 0.406 \cdot \ln C_e - 1.014$	0.990	$\frac{C_e}{q_e} = 0.481 \cdot C_e + 4.070$	0.967	2.078
45	$\ln q_e = 0.586 \cdot \ln C_e - 1.390$	0.994	$\frac{C_e}{q_e} = 0.341 \cdot C_e + 5.229$	0.948	2.933



Scheme 1. Protonation of the amino groups of chitosan hydrogel beads.

high concentration of  $H^+$  at low pH will drive the equilibrium to the right and therefore lead to an increased number of protonated amino sites, and further force Scheme 2 shift to left (A stands for FA). As a result, the adsorption of FA on the chitosan hydrogel beads decreases with increasing solution pH value. On the other hand, due to the existence of carboxylic and phenolic groups in its structure and their deprotonation [1], FA had negative charge for all pH studied. At lower pH more protons will be available to protonate amine groups of chitosan molecules to form groups  $-NH_3^+$  [30,31], thereby increasing electrostatic attractions between FA and adsorption sites and causing the observed increase in FA adsorption. As a result, adsorption capacity of FA is high in an acidic environment. Considering the PZC value of 9.9, the substantial decline in the adsorption capacity over pH 9 can be attributed to the reverse of the charge of chitosan hydrogel beads from positive to negative and the electrostatic interactions between FA and chitosan hydrogel beads changed from favorable to unfavorable.

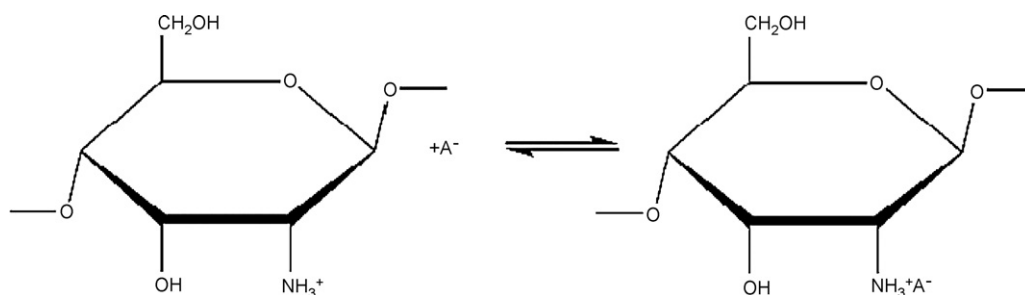
Moreover, at low pH, the FA macromolecules exist as partly or fully undissociated/protonated forms. The FA structure becomes more hydrophobic and thus more adsorbable onto chitosan hydrogel beads. On the other hand, at high pH, the inter- and intra-molecular electrostatic repulsive interactions become more important among the FA macromolecules and the FA becomes less hydrophobic. The FA molecules are dissociated and exist as torus- or ring-like structures [32]; the solubility of FA also increases [33]. Thus, less FA adsorption is observed.

The relationship between the initial and final pH of FA reacted chitosan hydrogel beads (Fig. 6) shows that the initial pH of 3.98 increased to 7.54, whereas an initial pH of 9.05 decreased to 7.76. An examination of the solution pH values indicated that the final solution pH values after the adsorption experiments increased under acidic adsorption conditions but decreased under basic adsorption conditions, as compared with the initial solution pH

values. However, with an initial pH of around 5.0–9.0, a stable pH zone was formed because a very insignificant change of pH occurred in that region. This may be due to the continuous protonation and deprotonation of chitosan hydrogel beads in the acidic and basic conditions.

### 3.6. Effect of ionic strength

The ionic strength of the solution is of significance for its effect on the adsorbent, as well as the adsorbate. In general, as different kinds of salts are mixed in real wastewater, its ionic strength is high [34]. To investigate the effect of ionic strength on FA adsorption, equilibrium sorption studies were carried out at different ionic strength. As expected, it was found that the amount of FA adsorbed onto chitosan hydrogel beads was a function of ionic strength, as shown in Fig. 7. The solid points represent the experimentally measured results, and the lines represent the results obtained by model calculations. In general, ionic strength had a positive effect on adsorption capacity of chitosan hydrogel beads at aqueous solution concentrations  $>30$  mg/L. According to Ghosh and Schnitzer [35], the configuration of dissolved FA is affected by ionic strength. At high ionic strength, the charge repulsion between adjacent carboxyl or hydroxyl groups on FA is largely neutralized, resulting in a coiled configuration [36]. The coiled FA may adsorb with fewer attachment points relative to its uncoiled configuration [29]. As a result, each FA molecule occupies less surface area resulting in a higher sorption density [29,37]. In addition, the colloidal chemistry theory [38] and the Derjaugin, Landau, Verwey, and Overbeek (DLVO) theory [39] indicated that at low ionic strength, FA has extended electric double layers, but as described by the DLVO theory, the double layer becomes compressed at high ionic strength, reducing the surface potential, but keeping the surface charge density constant. The compression of



Scheme 2. Adsorption of FA onto chitosan hydrogel beads.

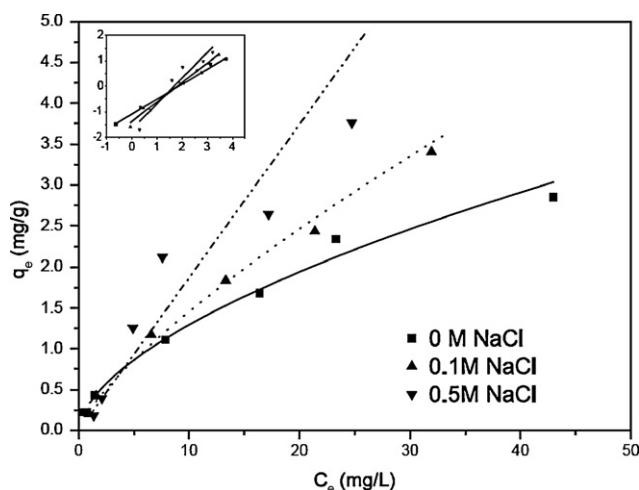


Fig. 7. Effect of ionic strength on the FA adsorption capacities of chitosan hydrogel beads.

the double layer results in a closer approach of FA and adsorbent which increases the adsorption capacity.

However, as shown in Fig. 7, at aqueous solution concentrations  $<30$  mg/L, the effect of ionic strength on FA adsorption is reversed; i.e., adsorption decreases with increasing ionic strength from 0 to 0.5 M NaCl, which indicated the intersection point of the isotherms marks the transition from the screening reduced to the screening enhanced adsorption mode. That is possible because that at low concentration adsorption is probably dependent on many factors such as surface charge, pore structure, surface chemistry, position, and concentration of charged and uncharged functional groups. It is also possible for that the excess positive charge may be located in regions inaccessible to the FA, i.e., the primary micropore region.

The ionic strength effects on the adsorption of FA reported in the literature are not consistent. Bjelopavlic investigated similar ionic strength effects of our study during adsorption of NOM onto activated carbon [40]. Whereas Schlautman and Morgan [41] have found that the adsorption of FA on aluminum oxides increases with increasing ionic strength and Vreysen and Maes [42] have found hardly any influence of the ionic strength on the adsorption of FA on bentonites.

### 3.7. Adsorption mechanisms

FTIR spectra have been a useful tool in identifying the presence of certain functional groups in a molecule as each specific chemical bond often shows a unique energy absorption band [40]. Fig. 8 shows the FTIR spectra of chitosan hydrogel beads before and after FA adsorption. Although the broad and strong band ranging from  $3200$  to  $3600$   $\text{cm}^{-1}$  may be due to the overlapping of  $-\text{OH}$  and  $-\text{NH}$  stretching, the strong broad band at the wavenumber region of  $3300$ – $3500$   $\text{cm}^{-1}$  is characteristic of the  $-\text{NH}$  stretching vibration. The absorption bands at  $\sim 1150$  (asymmetric stretching of the COC bridge),  $\sim 1080$ , and  $\sim 1030$  (skeletal vibrations involving  $-\text{CO}-$  stretching)  $\text{cm}^{-1}$  are characteristic of chitosan's saccharide structure [43,44]. In addition, the bands at peaks of  $1592$   $\text{cm}^{-1}$  for chitosan hydro-

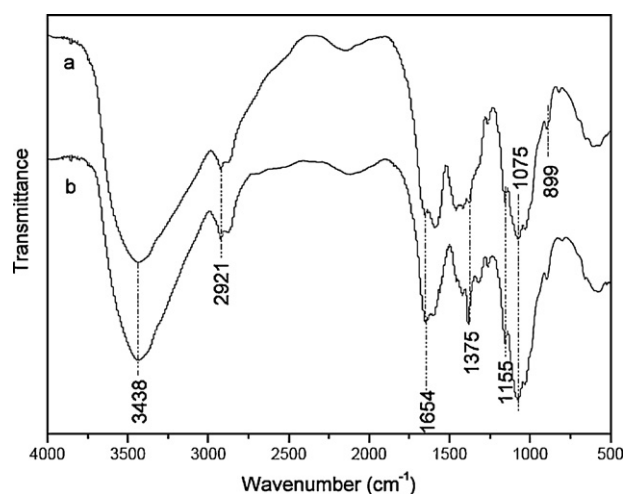


Fig. 8. FTIR spectra for chitosan hydrogel beads (a) before and (b) after FA adsorption.

gel beads can be assigned to the  $-\text{NH}$  group in amine [15], with the presence of this group being confirmed occurring at  $1419$   $\text{cm}^{-1}$  (which may be related to the presence of  $-\text{NH}_2$  groups). Significant changes in the FTIR spectra are found at the wavenumbers of  $1457$  and  $1375$   $\text{cm}^{-1}$  after FA adsorption. The peaks at the wavenumbers of  $1457$  and  $1375$   $\text{cm}^{-1}$  can be assigned to the  $-\text{NH}$  deformation vibration and  $-\text{CN}-$  stretching vibration in chitosan hydrogel bead molecules, respectively. The significant decrease of transmittance in the band region of  $3200$ – $3600$   $\text{cm}^{-1}$  after FA adsorption indicates that the  $-\text{NH}$  vibration was affected due to FA adsorption. Other changes in the transmittances can be observed at the wavenumbers of  $1654$ ,  $1592$ ,  $1375$ , and  $899$   $\text{cm}^{-1}$ , respectively. These wavenumbers are closely related to the  $-\text{NH}$  bending,  $-\text{CN}-$  stretching and  $-\text{NH}$  rocking bands. In other words, FA adsorption is found to affect all of the bonds with N atoms, indicating that nitrogen atoms are the main adsorption sites for FA adsorption on chitosan hydrogel beads. Another major change in the transmittance can also be observed at the wavenumber of  $2921$   $\text{cm}^{-1}$ . This band region may be assigned to both  $-\text{CH}$  (variable) and  $-\text{OH}$  (weak-broad) stretchings. As FA is unlikely to be attached to a carbon atom, the results may therefore suggest that oxygen atoms in the hydroxyls could also be involved in FA adsorption, but their effect appears to be much less significant than nitrogen atoms.

To further investigate the interactions between FA and chitosan hydrogel beads and the attachment mechanisms of FA on the chitosan hydrogel beads, XPS studies of the chitosan hydrogel beads before and after FA adsorption at pH 4 were conducted. Fig. 9 shows the N 1s core-level spectra of chitosan hydrogel beads before and after FA adsorption, respectively. As shown in Fig. 9a, the N 1s spectrum has only a single peak located at a binding energy (BE) of  $399.2$  eV, corresponding to the neutral amine nitrogen ( $-\text{NH}$  or  $-\text{NH}_2$ ) in chitosan hydrogel beads. However, when chitosan hydrogel beads were placed into FA solution, a higher binding energy peak at  $400.4$  eV appeared, indicating the generation of  $-\text{NH}_3^+$  as a result of interaction between the amino groups in chitosan hydrogel beads and the adsorbed FA. This result indicates that FA coordinated to the

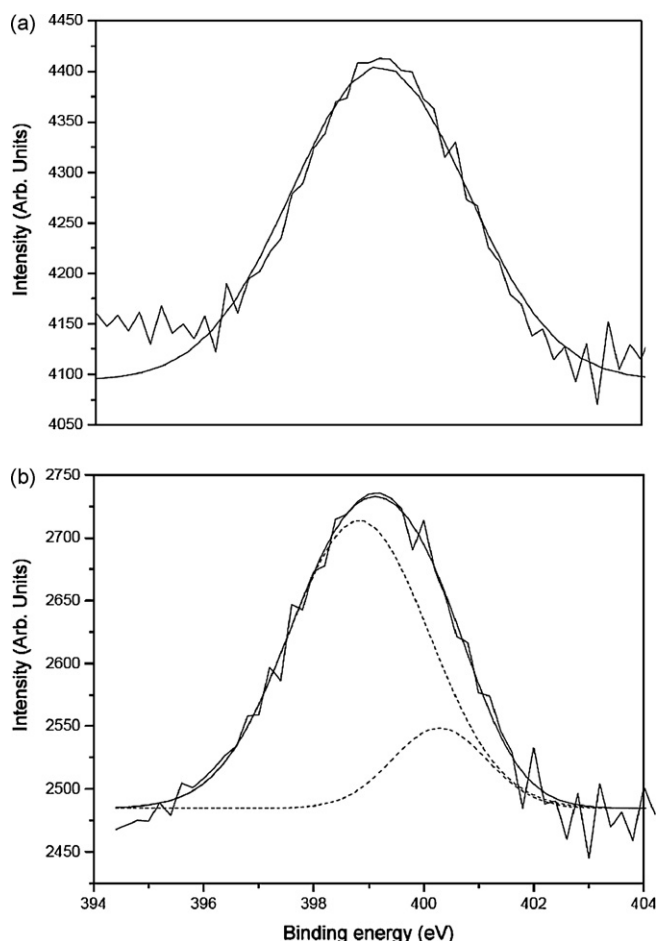


Fig. 9. N 1s core spectra of (a) before and (b) after FA adsorption.

amine site on chitosan hydrogel beads surface, resulting in the lone electron pair of the nitrogen atom being shared by the attached  $A^+$  species, and thus giving a higher BE in the N 1s spectrum for the more oxidized nitrogen  $-NH_3^+$  [45]. It is consistent with the findings of earlier studies, which proposed that the amino groups on the adsorbent were protonated and subsequently interacted with the carboxyl or phenolic groups in humic acid to form the organic complexes [46,47]. The proportion of the uncharged nitrogen atoms in  $-NH_2$  or  $-NH$  to the positively charged nitrogen atoms on the surface of chitosan hydrogel beads is found to be 0.18. In conclusion, the above analysis reveals that the FA adsorption mechanism onto chitosan hydrogel beads can be viewed as the complexation of the negative functional groups (such as unprotonated carboxyl, phenolic groups) in FA with the positive functional groups (protonated amino groups) onto chitosan hydrogel beads.

#### 4. Conclusions

This study examined the behaviors and mechanisms of chitosan hydrogel beads as an adsorbent to remove FA from aqueous solution. The study clearly confirms that chitosan hydrogel beads have a potential in applications of separation of FA. The obtained results may be summarized as follows:

- The adsorption of FA was highly dependent on initial concentration, pH, ionic strength and temperature. The present work confirmed the existence of intersection point in the adsorption isotherms undertaken at three ionic strengths which were indicative of a change in the adsorption mechanism from the screening reduced to the screening enhanced modes. The FA adsorption capacity increased with the increase of pH in the range of 4–12.
- The adsorption kinetic and isotherm study showed that the adsorption processes were fitted well with the intra-particle model and the Freundlich equation, respectively.
- FTIR and XPS analysis revealed that the amino groups of chitosan hydrogel beads in a protonated state, which can form the surface complex with FA, were found to play the major role in the adsorption process.

#### References

- [1] L. Zhao, F. Luo, J.M. Wasikiewicz, H. Mitomo, N. Nagasawa, T. Yagi, M. Tamada, F. Yoshii, Adsorption of humic acid from aqueous solution onto irradiation-crosslinked carboxymethylchitosan, *Bioresour. Technol.* 99 (2008) 1911–1917.
- [2] Y.Ş. Yıldız, A.S. Koparal, B. Keskinler, Effect of initial pH and supporting electrolyte on the treatment of water containing high concentration of humic substances by electrocoagulation, *Chem. Eng. J.* 138 (2008) 63–72.
- [3] J.F. Fu, M. Ji, Y.Q. Zhao, L.Z. Wang, Kinetics of aqueous photocatalytic oxidation of fulvic acids in a photocatalysis-ultrafiltration reactor (PUR), *Sep. Purif. Technol.* 50 (2006) 107–113.
- [4] S.G. Wang, W.X. Gong, X.W. Liu, B.Y. Gao, Q.Y. Yue, Removal of fulvic acids using the surfactant modified zeolite in a fixed-bed reactor, *Sep. Purif. Technol.* 51 (2006) 367–373.
- [5] H. Galland, U.V. Gunten, Chlorination of natural organic matter: kinetics of chlorination and of THM formation, *Water Res.* 36 (2002) 65–74.
- [6] S.G. Wang, X.W. Liu, W.X. Gong, W. Nie, B.Y. Gao, Q.Y. Yue, Adsorption of fulvic acids from aqueous solutions by carbon nanotubes, *J. Chem. Tech. Biotechnol.* 82 (2007) 698–704.
- [7] C. Jucker, M.M. Clark, Adsorption of aquatic humic substances on hydrophobic ultrafiltration membranes, *J. Membr. Sci.* 97 (1994) 37–52.
- [8] B. Bolto, D. Dixon, Removal of natural organic matter by ion exchange, *Water Res.* 36 (2002) 5057–5065.
- [9] E. Aoustin, A.I. Schäfer, A.G. Fane, T.D. Waite, Ultrafiltration of natural organic matter, *Sep. Purif. Technol.* 22–23 (2001) 63–78.
- [10] J.Q. Jiang, C. Cooper, Preparation of modified clay adsorbents for the removal of humic acid, *Environ. Eng. Sci.* 20 (2003) 581–586.
- [11] T. Karanfil, M.A. Schlautman, J.W. Weber Jr., Impacts of dissolved oxygen on the sorption of humic substances and the subsequent inhibition of *o*-cresol uptake by granular activated carbon, *Water Res.* 28 (1994) 1673–1678.
- [12] M.A. Schlautman, J.J. Morgan, Adsorption of aquatic humic substances on colloidal-size aluminum oxide particles: influence of solution chemistry, *Geochim. Cosmochim. Acta* 58 (1994) 4293–4303.
- [13] Y. Seida, Y. Nakano, Removal of humic substances by layered double hydroxide containing iron, *Water Res.* 34 (2000) 1487–1494.
- [14] S.P. Kamble, S. Jagtap, N.K. Labhsetwar, D. Thakare, S. Godfrey, S. Devotta, S.S. Rayalu, Defluoridation of drinking water using chitin, chitosan and lanthanum-modified chitosan, *Chem. Eng. J.* 129 (2006) 173–180.
- [15] N.K. Lazaridis, G.Z. Kyzas, A.A. Vassiliou, D.N. Bikiaris, Chitosan derivatives as biosorbents for basic dyes, *Langmuir* 23 (2007) 7634–7643.
- [16] Y.C. Wong, Y.S. Szeto, W.H. Cheung, G. McKay, Equilibrium studies for acid dye adsorption onto chitosan, *Langmuir* 19 (2003) 7888–7894.
- [17] W.S. Wan Ngah, K.H. Liang, Adsorption of gold (III) ions onto chitosan and *N*-carboxymethyl chitosan: equilibrium studies, *Ind. Eng. Chem. Res.* 38 (1999) 1411–1414.



- [18] R. Johanna, W.G. Evans, J.D. Davids, A. Mac Rae, Kinetics of cadmium uptake by chitosan-based crab shells, *Water Res.* 36 (2002) 3219–3226.
- [19] A. Shafaei, F.Z. Ashtiani, T. Kaghazchi, Equilibrium studies of the sorption of Hg(II) ions onto chitosan, *Chem. Eng. J.* 133 (2007) 311–316.
- [20] B.M. Babić, S.K. Milonjić, M.J. Polovina, B.V. Kaludierović, Point of zero charge and intrinsic equilibrium constants of activated carbon cloth, *Carbon* 37 (1999) 477–481.
- [21] J.P. Wang, Y.Z. Chen, H.M. Feng, S.J. Zhang, H.Q. Yu, Removal of 2,4-dichlorophenol from aqueous solution by static-air-activated carbon fibers, *J. Colloid Interf. Sci.* 313 (2007) 80–85.
- [22] W.S.W. Ngah, A. Musa, Adsorption of humic acid onto chitin and chitosan, *J. Appl. Polym. Sci.* 69 (1998) 2305–2310.
- [23] B.H. Hameed, A.A. Ahmad, N. Aziz, Isotherms, kinetics and thermodynamics of acid dye adsorption on activated palm ash, *Chem. Eng. J.* 133 (2007) 195–203.
- [24] A.K. Bhattacharya, T.K. Naiya, S.N. Mondal, S.K. Das, Adsorption, kinetics and equilibrium studies on removal of Cr(VI) from aqueous solutions using different low-cost adsorbents, *Chem. Eng. J.* 137 (2008) 529–541.
- [25] M.Y. Chang, R.S. Juang, Adsorption of tannic acid, humic acid, and dyes from water using the composite of chitosan and activated clay, *J. Colloid Interf. Sci.* 278 (2004) 18–25.
- [26] A. Meghea, H.H. Rehner, I. Peleanu, R. Mihalache, Test-fitting on adsorption isotherms of organic pollutants from waste waters on activated carbon, *J. Radioanal. Nucl. Chem.* 229 (1998) 105–110.
- [27] L. Wang, Y.P. Chin, S.J. Traina, Adsorption of (poly) maleic acid and an aquatic fulvic acid by goethite, *Geochim. Cosmochim. Acta* 61 (1997) 5313–5324.
- [28] M.M. Ramos-Tejada, A. Ontiveros, J.L. Viota, J.D.G. Durán, Interfacial and rheological properties of humic acid/hematite suspensions, *J. Colloid Interf. Sci.* 268 (2003) 85–95.
- [29] E.M. Murphy, J.M. Zachara, S.C. Smith, Interfacial and rheological properties of humic acid/hematite suspensions, *Environ. Sci. Technol.* 24 (1990) 1507–1516.
- [30] M. Hasan, A.L. Ahmad, B.H. Hameed, Adsorption of reactive dye onto cross-linked chitosan/oil palm ash composite beads, *Chem. Eng. J.* 136 (2008) 164–172.
- [31] M.N.V. Ravi Kumar, A review of chitin and chitosan applications, *React. Funct. Polym.* 46 (2000) 1–27.
- [32] M. Plaschke, J. Römer, R. Klenze, J.I. Kim, In situ AFM study of sorbed humic acid colloids at different pH, *Colloids Surf. A-Phys. Eng. Aspects* 160 (1999) 269–279.
- [33] J.L. Zhou, S. Rowland, R.F.C. Mantoura, J. Braven, The formation of humic coatings on mineral particles under simulated estuarine conditions—a mechanistic study, *Water Res.* 28 (1994) 571–579.
- [34] G.J. Ramelow, D. Fralick, Y. Zhao, Factors affecting the uptake of aqueous metal ions by dried seaweed biomass, *Microbios.* 72 (1992) 81–93.
- [35] K. Ghosh, M.J. Schnitzer, UV and visible absorption spectroscopic investigations in relation to macromolecular characteristics of humic substances, *Soil Sci.* 30 (1979) 735–745.
- [36] E. Tipping, D. Cooke, The effects of adsorbed humic substances on the surface charge of goethite ( $\alpha$ -FeOOH) in freshwaters, *Geochim. Cosmochim. Acta* 46 (1982) 75–80.
- [37] E.M. Murphy, J.M. Zachara, S.C. Smith, J.L. Phillips, T.W. Wietsma, In situ AFM study of sorbed humic acid colloids at different pH, *Environ. Sci. Technol.* 28 (1994) 1291–1299.
- [38] C.J. Banks, M.E. Parkinson, The mechanism and application of fungal biosorption to color removal from raw waters, *J. Chem. Tech. Biotechnol.* 54 (1992) 192–196.
- [39] W. Stumm, J.J. Morgan, *Aquatic Chemistry: an Introduction Emphasizing Chemical Equilibria in Natural Waters*, Wiley-Interscience, New York, NY, USA, 1981, pp. 599–684.
- [40] M. Bjelopavlic, G. Newcombe, R. Hayes, Adsorption of NOM onto activated carbon: effect of surface charge, ionic strength, and pore volume distribution, *J. Colloid Interf. Sci.* 210 (1999) 271–280.
- [41] M.A. Schlautman, J.J. Morgan, Adsorption of aquatic humic substances on colloidal-size aluminum-oxide particles influence of solution chemistry, *Geochim. Cosmochim.* 58 (1994) 4293–4303.
- [42] S. Vreysen, A. Maes, Adsorption mechanism of fulvic acid onto freeze dried poly (hydroxo aluminum) intercalated bentonites, *Appl. Clay Sci.* 32 (2006) 190–196.
- [43] A.L.P. Fernandes, W.A. Morais, A.I.P. Santos, A.M.L. de Araujo, D.E.S. dos Santos, D.S. dos Santos, F.J. Pavinatto, O.N. Oliveira, T.N.C. Dantas, M.R. Pereira, J.L.C. Fonseca, The influence of oxidative degradation on the preparation of chitosan nanoparticles, *Colloid Polym. Sci.* 284 (2005) 1–9.
- [44] C.L. de Vasconcelos, B.M. Bezerril, D.E.S. dos Santos, T.N.C. Dantas, M.R. Pereira, J.L.C. Fonseca, Effect of molecular weight and ionic strength on the formation of polyelectrolyte complexes based on poly (methacrylic acid) and chitosan, *Biomacromolecules* 7 (2006) 1245–1252.
- [45] A.K. Arof, N.M. Morni, M.A. Yarmo, Evidence of lithium-nitrogen interaction in chitosan-based films from X-ray photoelectron spectroscopy, *Mater. Sci. Eng. B* 55 (1998) 130–133.
- [46] X. Zhang, R. Bai, Mechanisms and kinetics of humic acid adsorption onto chitosan-coated granules, *J. Colloid Interf. Sci.* 264 (2003) 30–38.
- [47] S. Deng, R. Bai, Aminated polyacrylonitrile fibers for humic acid adsorption: behaviors and mechanisms, *Environ. Sci. Technol.* 37 (2003) 5799–5805.